A [Fe III (Tp)(CN) 3] – scorpionate-based complex as a building block for designing ion storage hosts (Tp: hydrotrispyrazolylborate)

Juan-Ramón Jiménez, Akira Sugahara, Masashi Okubo, Atsuo Yamada, Lise-Marie Chamoreau, Laurent Lisnard, Rodrigue Lescouëzec

$[Fe^{III}(Tp)(CN)_3]^-$ Scorpionate-based Complex as a Building Block for designing Ion-Storage Hosts (Tp: hydrotrispyrazolylborate)

Juan Ramon Jimenez,[a] Akira Sugahara,[b] Masashi Okubo,[b] Atsuo Yamada,[b] Lise-Marie Chamoreau,[a] Laurent Lisnard,[a] Rodrigue Lescouëzec [a,*]

Using a scorpionate-based complex, $[Fe^{III}(Tp)(CN)_3]^-$, as a bulding block, a new cyanide-based molecular material $[\{Fe^{III}(Tp)(CN)_3\}_2Ni^{II}(H_2O)_2]\cdot 4H_2O$ (1), which can be viewed as a lower dimensional model of Prussian blue analogues, was investigated as a lithium-ion storage host.

The molecular self-assembly of preformed complexes in soft conditions is an interesting alternative to more energy-consuming routes generally used in solid-state chemistry in order to obtain functional materials. In recent years, strong research efforts have been devoted to the design of functional coordination polymers and metal organic frameworks.[1] Cyanide coordination chemistry nicely illustrates the efficiency of the self-assembly synthetic approach. In fact, the existence of numerous stable polycyanido-metallates $[M(CN)_n]^{m-}$ building blocks (M: transition metal), allows the tuning of the electronic properties and the architecture of the resulting self-assembled materials.[2] The strength of the M-CN-M' bridges can also confer structural robustness to the obtained networks. Finally, the cyanide bridges promote efficient electronic couplings between the metal ions it links, which can lead to interesting magnetic, optical or electronic properties.[3] In this context, a large number of Prussian Blue Analogues (PBAs) and cyanide-bridged frameworks have been studied for many kinds of application including catalysis,[4] bio-sensing,[5] gas storage,[6] etc.

The use of cyanido complexes, $[M(L)(CN)_n]^{m-}$, which contain ancillary ligand (L), has permitted the preparation of new architectures, in particular the design of molecular materials that exhibit reduced dimensionality.[7] The *fac*-$[Fe^{III}(Tp)(CN)_3]^-$ complex (Tp: hydrotris(pyrazolyl)borate) that we first described in 2002 has been particularly used in this context.[8] The Tp^- ligand belongs to the well-known scorpionate ligand family that can be easily functionalized,[9] allowing the adjustment of its electronic and steric properties. This anisotropic building block[10] has proven to be very useful to prepare low-dimensional molecular materials such as single molecule magnets, switchable and multifunctional materials.[11]

In the present work, we wish to explore the potentialities of cyanide-based materials, especially a $[Fe^{III}(Tp)(CN)_3]$-based framework as ion storage hosts, which are applicable to electrochemical devices such as electrochromic devices and batteries. Although application of PBAs to batteries has recently attracted much attention,[12] only a few examples of ion storage in other cyanide-based materials have been reported.[13]

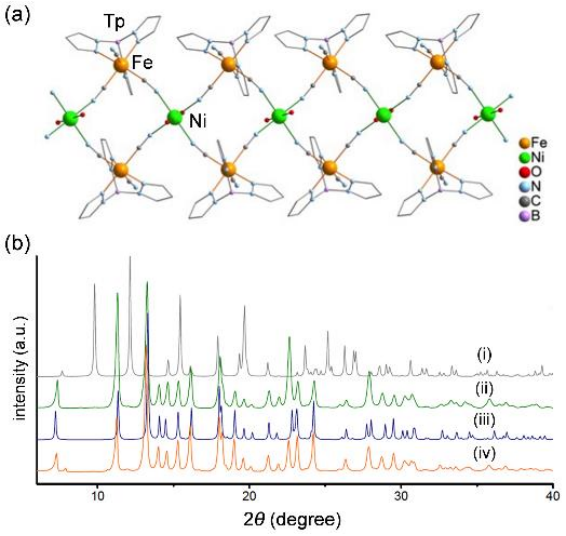

Figure 1. (a) Perspective view of the crystal structure of **1**. (b) (i) Calculated powder X-ray diffraction pattern from the single-crystal structure of **1'** (grey). (ii) Experimental powder X-ray diffraction pattern of the air-dried crystals of **1'** (green). (iii) Calculated powder X-ray diffraction pattern from the single-crystal structure of **1** (blue). (iv) Experimental powder X-ray diffraction pattern of the directly precipitated powder (orange).

In this paper, we selected as a model compound a simple and known one dimensional (1D) material of formula $\{[Fe^{III}(Tp)(CN)_3]_2[Ni^{II}(H_2O)_2]\}_n$, which contains the versatile $[Fe^{III/II}(Tp)(CN)_3]^-$ building block. We expected that, while this building block exhibits a higher redox potential relative to the parent $[Fe^{III/II}(CN)_6]^{3-/4-}$, which could lead to higher reaction voltage, the lower dimensionality and open framework should confer more flexibility to the framework and more space to permit easier ion (de)intercalation. The questions we wanted to address were as follows: are lower dimensional cyanide-based materials still robust enough to reversibly insert alkali ions? Is the electronic conductivity of the 1D material high enough (compare to 3D phases) for it to act as a cathode? Can the scorpionate-based subunits be reversibly oxidized/reduced in the solid state? We thus report here the electrochemical Li^+ (de)intercalation properties of the $\{[Fe(Tp)(CN)_3]_2[Ni(H_2O)_2]\}$ chain compound.

The 1D cyanide-bridged compound $\{[Fe^{III}(Tp)(CN)_3]_2[Ni^{II}(H_2O)_2]\}\cdot 4H_2O$ (**1**) was obtained by direct precipitation in CH_3OH/H_2O (7/3 mixture) upon reacting $NBu_4[Fe^{III}(Tp)(CN)_3]$ with $Ni(NO_3)_2\cdot 6H_2O$. The powder XRD pattern of the resulting microcrystalline compound (Fig. 1b,

orange) shows that its structure differs from the initially targeted material ({[Fe^{III}(Tp)$(CN)_3$]$_2$[$Ni^{II}(CH_3OH)_2$]}·CH_3OH 0.5H_2O (**1'**), Fig. 1b, grey) that was previously reported by You *et al*.[14] The hydrated compound **1** can also be obtained by a single-crystal to single-crystal phase transition. The XRD analysis revealed that methanol in the single crystal of **1'** is completely replaced by water after 3 days in ambient atmosphere to give **1** (Fig. S1, supporting information). The calculated XRD pattern based on the crystal structure of **1** matches the pattern measured for the precipitated material (Fig. 1b, blue).

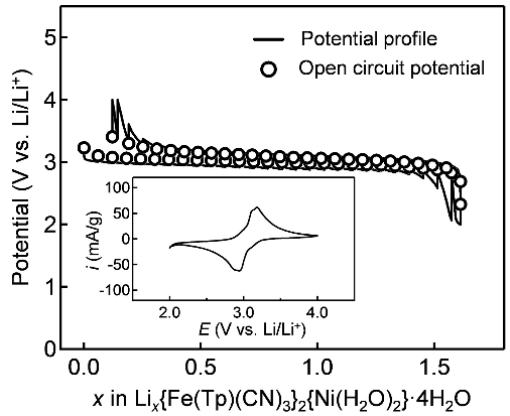

Figure 2. Open circuit potentials of **1** in a 1M $LiClO_4$/PC electrolyte. The inset shows the cyclic voltammetry during the second cycle at the scan rate of 0.2 mV/s.

Despite the change of the solvent molecules coordinating to the Ni(II) ion, the structure of **1** is very similar to that of **1'**. It consists of $Fe^{III}_2Ni^{II}$ neutral chains made of cyanide-bridged $Fe^{III}_2Ni^{II}_2$ squares. The cyanide bridges are almost linear and the Fe-Ni distances (5.022(3) and 5.076(3) Å) are very similar to that found in the parent $Ni_3[Fe(CN)_6]_2$ PBA (ca. 5.05 Å). In fact, the FT-IR spectra (see supporting information) exhibit intense cyanide stretching vibrations at 2164 cm^{-1} and 2167 cm^{-1}, characteristic of bridging Fe^{III}-CN-Ni^{II}. The $Fe^{III}_2Ni^{II}_2$ squares are connected to each other by the Ni(II) vertices and form the 1D material. The Fe(III) ions are coordinated by a Tp^- ligand in a facial mode. Three other coordination sites are occupied by the carbon atoms of three cyanide ligands. The coordination sphere of the Ni(II) ion is made of four nitrogen atoms from the cyanide ligands and two oxygen atoms from two coordinated water molecules, so the coordination surrounding of the divalent atom is similar to that found on average in the lacunary $M^{II}_3[Fe^{III}(CN)_6]_2$.[15] The chains are separated from each other by the organic shell constituted by the pyrazolyl rings of the Tp ligands. However, the hydrogen-bond network involving the coordinated and non-coordinated water molecules (Fig. S4, Supporting Information) links the adjacent chains to each other and leads to a contraction of the unit cell along the *b* crystallographic axis as compared to the You's material (**1'**).

The cyclic voltammetry (CV) was carried out to clarify the solid-state electrochemical property of **1** in a non-aqueous Li^+ electrolyte. The CV curve recorded at the sweep rate of 0.2 mV/s (inset in Fig. 2) exhibits a reversible pair of cathodic/anodic current waves with small polarization (a peak-to-peak separation of approximately 0.24 V). The redox potential (the average of the cathodic/anodic-peak potentials) is 3.06 V vs. Li/Li^+ (-0.23 V vs. SCE), which is slightly lower than that observed in $Ni_3[Fe(CN)_6]_2$ PBA (3.30 V vs. Li/Li^+, *i.e.*, 0.02 V vs. SCE).

The redox potential of the $[Fe^{III/II}(Tp)(CN)_3]^{-/2-}$ building block, in organic solvent is higher than that of the $[Fe^{III/II}(CN)_6]^{3-/4-}$ complex (-0.61 V and -1.06 V vs SCE in CH_3CN, respectively).[16] These values increase upon coordination of divalent metal ion to the nitrogen atom of the cyanide ligands. For example, in the $[Fe^{III}_4(Tp)_4Ni^{II}_4(NMe_2Tp)_4(CN)_{12}]$ complex, the first $Fe^{III/II}$ redox potential moves up to +0.09V *vs* SCE in CH_3CN, a shift of +0.7 V compared to the $[Fe^{III/II}(Tp)(CN)_3]^{-/2-}$ complex.[17] The redox potential shift of $\{Fe^{III/II}(Tp)(CN)_3\}^{-/2-}$ units contained in **1** (+0.38 V in comparison to the $[Fe^{III/II}(Tp)(CN)_3]^{-/2-}$), is not so large as only two nickel are coordinated to two cyanide. The shift is larger for the $\{Fe(CN)_6\}^{3-}$ subunits contained in the Ni-Fe PBAs (+1.08 V) as the iron complex is linked through six cyanide bridges to six Ni(II) ions (only two in the 1D material). Overall this leads to similar redox potentials in the 1D and the 3D materials.

The electrochemical Li^+ (de)intercalation in **1** was further evaluated galvanostatically. The open circuit potentials (Fig. 2) indicate that reversible (de)intercalation of approximately 1.6 Li^+ occurs per the Fe_2Ni unit. Some defects or side reactions occurring at the surface of the material are likely to prevent the complete reduction of Fe^{III}.[12] However, most of the $\{Fe^{III}(Tp)(CN)_3\}^-$ units in the pristine compound undergoes reversible redox reaction associated with Li^+ (de)intercalation. Indeed, X-ray absorption near edge structure (XANES) spectroscopy shows that the main peak position of the Fe *K*-edge shifts to lower energy after Li^+ intercalation, and shifts back to the original position after Li^+ deintercalation (Fig. 3a). The XANES spectra at the Ni *K*-edge do not show any shift of the main peak position during Li^+ (de)intercalation (Fig. 3b). These results confirm that the reversible redox reaction in **1** occurs on the $[Fe^{III/II}(Tp)(CN)_3]^{-/2-}$ building block. To the best of our knowledge, this result is the first demonstration of a reversible Li^+ (de)intercalation in a 1D cyanide-bridged molecular material obtained by self-assembly of preformed building blocks.

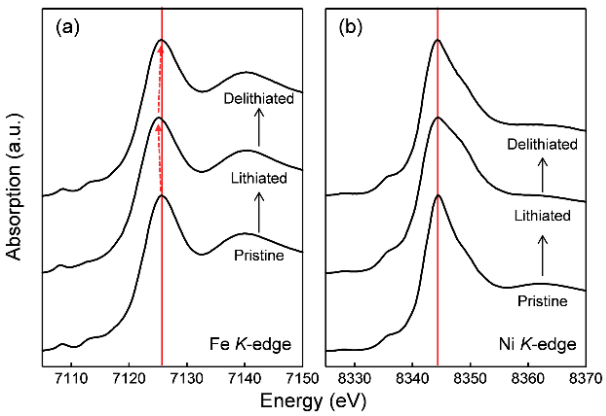

Figure 3. Ex situ X-ray absorption spectra for (a) Fe and (b) Ni K-edges of **1** upon (de)lithiation.

The ex-situ XRD measurements for (de)lithiated compounds were conducted to clarify the structural change (Fig. S5, supporting information). The ex-situ XRD pattern for the lithiated compound does not show diffraction peaks, indicating the loss of crystallinity. A similar behaviour was also observed for a 2D cyanide-bridged compound $\{Tb(H_2O)_5[W(CN)_8]\}$.[18] Presumably, the interchain interaction (mostly hydrogen bonds) is weak relative to the Madelung potential change of Li^+ intercalation and Fe reduction, leading to the loss of the long-range stacking of the 1D chains. However, as discussed below, the 1D framework is maintained during the Li^+ (de)intercalation to give good capacity retention over 50 cycles (Fig. S6, supporting information).

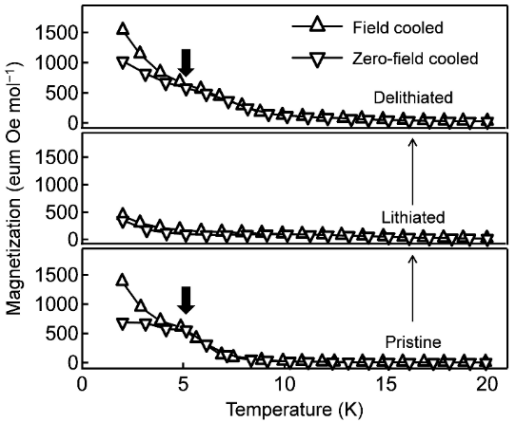

Figure 4. Magnetic property changes of **1** upon (de)lithiation. The black arrows indicate the ferromagnetic transition temperature.

The magnetic measurements before and after Li^+ (de)intercalation were studied using ex-situ SQUID measurements (Fig. 4). The observed magnetic behaviour of **1** (Fig. S7-S9, supporting information) is typical of a ferromagnetic chain. The observed ferromagnetic coupling is as predicted on the basis of simple orbital symmetry consideration: the unpaired electron of the iron(III) centre is described by a t_{2g} type magnetic orbital (π symmetry) whereas the two unpaired electrons of the nickel(II) centre are in two e_g orbitals (σ symmetry). The Field-Cooled and Zero-Field Cooled magnetization (FC-ZFC) curves (Fig. 4 and S7) indicate the occurrence of magnetic ordering at 5 K due to interchains interactions. Overall, the magnetic properties of the pristine compound **1** are similar to those observed for **1'** reported by You *et al*.[14]

After 1.6 Li^+ intercalation per $\{Fe_2Ni\}$ unit, most paramagnetic low-spin Fe^{III} ions are reduced to diamagnetic low-spin Fe^{II}. Therefore, the material does not behave as a ferromagnetic chain and the magnetic order disappears.[19] Indeed, the FC-ZFC curves for the lithiated sample (Fig. 4) do not show an abrupt increase of magnetization, indicating the disappearance of the magnetic order. Importantly, the ferromagnetic transition occurring at 5 K is recovered after Li^+ deintercalation. This shows that the material still behaves as interacting ferromagnetic chains, and thus the 1D Fe_2Ni framework is maintained, even though electrochemical Li^+ intercalation induces the loss of the crystallinity. The Fe *K*-edge extended X-ray fine structure (EXAFS) spectra before and after Li^+ intercalation (Fig. S10, supporting information) also indicate that the Fe coordination sphere is not significantly altered.

In summary, we have shown that our synthetic approach based on the self-assembly of tailored cyanide building blocks in soft conditions is valid to obtain molecular material capable of ion storage. The $[Fe(Tp)(CN)_3]^-$ is a novel versatile building unit to design electrochemically-active molecule-based magnetic materials. We are now focusing our efforts on the use of modified Fe building blocks with higher redox potentials.

This work was financially supported by the ANR-JST Strategic International Collaborative Research Program (SICORP), Molecular Technology, Molecular Materials for Magnesium Batteries (MoMa). X-ray absorption spectroscopy was conducted under the approval of the Photon Factory Program Advisory Committee (Proposal 2016G031). We thank B. Baptiste from IMPMC for initial PXRD measurements.

Conflicts of interest

There are no conflicts to declare.

Notes and references

‡Electronic supplementary information (ESI) available: Experimental section, crystal structure, ex situ XRD patterns, magnetic properties, FT-IR, TGA, and EXAFS measurements.

1 *The Chemistry Metal Organic Frameworks: Synthesis, Characterization and Applications, Ed. S. Kaskel, Wiley VCH, 2016*
2 E. V. Alexandrov, A. V. Virovets, V. A. Blatov, E. V. Peresypkina, *Chem. Rev.* 2015, **115**, 12286.
3 S. Ohkoshi, H. Tokoro, *Acc. Chem. Res.* 2012, **45**, 1749.
4 S. Pintado, S. Goberna-Ferrón, E. Escudero-Adán, J.R. Galán-Mascarós, *J. Am. Chem. Soc.* 2013, **135**, 13270.
5 Advanced Biomaterials and Biodevices, Ed. A Tiwary, A. N. Nordin, Scrivener Pub.-Wiley, 2014.
6 S. S. Kaye, J. R. Long, *J. Am. Chem. Soc.* 2005, **127**, 6506.
7 R. Lescouëzec, L. Toma, J. Vaissermann, M. Verdaguer, F.S. Delgado, C. Ruiz-Perez, F. Lloret, M. Julve, *Coord. Chem. Rev.* 2005, **249**, 2691.
8 R. Lescouëzec, F. Lloret, M. Julve, J. Vaissermann, M. Verdaguer, *Inorg. Chem.* 2002, **41**, 5943.
9 Scorpionates II, chelating borate ligands, C. Pettinari, Imperial College Press, 2008.
10 K. Ridier, A. Mondal, C. Boilleau, O. Cador, B. Gillon, G. Chaboussant, B. Le Guennic, K. Costuas, R. Lescouëzec, *Angew. Chem. Int. Ed.* 2016, **55**, 3963;
11 (a) P. J. Ferko, S. M. Holmes, *Curr. Inorg. Chem.,* **2013**, 172. (b) D. Aguila, Y. Prado, E. Koumousis, C. Mathonière, R. Clérac, *Chem. Soc. Rev.* 2016, **45**, 203;
12 (a) N. Imanishi, T. Morikawa, J. Kondo, Y. Takeda, O. Yamamoto, N. Kinugasa, T. Yamagishi, *J. Power Sources*, 1999, **79**, 215. (b) M. Okubo, D. Asakura, Y. Mizuno, J. D. Kim, T. Mizokawa, T. Kudo, and I. Honma, *J. Phys. Chem. Lett.*,

2010, **1**, 2063; (c) C.D. Wessels, R.A. Huggins, Y. Cui, *Nat. Commun.*, 2011, 2550. (d) Y. H. Lu, L. Wang, J. B. Goodenough, *Chem. Commun.*, 2012, **48**, 6544. (e) L. Wang, J. Song, R. M. Qiao, L. A. Wray, M. A. Hossain, Y. D. Chuang, W. L. Yang, Y. H. Lu, D. Evans, J. J. Lee, S. Vail, X. Zhao, M. Nishijima, S. Kakimoto, J. B. Goodenough, *J. Am. Chem. Soc.*, 2015, **137**, 2548. (e) M. Okubo, C. H. Li, D. R. Talham, *Chem. Commun.*, 2014, **50**, 1353. (f) S. Kajiyama, Y. Mizuno, M. Okubo, R. Kurono, S. Nishimura, A. Yamada, *Inorg. Chem.* 2014, **53**, 3141. (g) D. Asakura, C. H. Li, Y. Mizuno, M. Okubo, H. S. Zhou, D. R. Talham, *J. Am. Chem. Soc.*, 2013, **135**, 2793.

13 M. Okubo, K. Kagesawa, Y. Mizuno, D. Asakura, E. Hosono, T. Kudo, H. S. Zhou, K. Fujii, H. Uekusa, S. Nishimura, A. Yamada, A. Okazawa, N. Kojima, *Inorg. Chem.*, 2013, **52**, 3772.

14 H.-R. Wen, C.-F. Wang, Y. Song, S. Gao, J.-L. Zuo, X. You, *Inorg. Chem.* 2006, **45**, 8942

15 A. Flambard, A. Sugahara, S. De, M. Okubo, A. Yamada, R. Lescouëzec, *Dalton Trans*, 2017, *46*, 6159

16 D. Garnier, J.-R. Jiménez, Y. Li, J. von Bardeleben, Y. Journaux, T. Augenstein, E. Moos, M. Gamer, F. Breher, R. Lescouëzec, *Chem. Sci.*, 2016, **7**, 4825.

17 R. Plamont, J. Tami, J.-R. Jimenez, A. Benchohra, O. Khaled, G. Gontard, Y. Li, R. Lescouëzec, *J. Coord. Chem.*, 2018, *accepted*.

18 J. Long, D. Asakura, M. Okubo, A. Yamada, Y. Guari, J. Larionova, *Inorg. Chem.* 2016, **55**, 7637.

19 (a) Y. Mizuno, M. Okubo, K. Kagesawa, D. Asakura, T. Kudo, H. S. Zhou, K. Oh-ishi, A. Okazawa, N. Kojima, *Inorg. Chem.*, 2012, **51**, 10311. (b) M. Okubo, D. Asakura, Y. Mizuno, T. Kudo, H. S. Zhou, A. Okazawa, N. Kojima, K. Ikedo, T. Mizokawa, I. Honma, *Angew. Chem. Int. Ed.*, 2011, **50**, 6269.